Sensors & Actuators: B. Chemical 296 (2019) 126688

Contents lists available at ScienceDirect

Sensors and Actuators B: Chemical

journal homepage: www.elsevier.com/locate/snb

Mixed potential type acetone sensor based on $Ce_{0.8}Gd_{0.2}O_{1.95}$ and $Bi_{0.5}La_{0.5}FeO_3$ sensing electrode used for the detection of diabetic ketosis

Tong Liu[a], Luyao Li[b], Xinyu Yang[a], Xishuang Liang[a,*], Fengmin Liu[a], Fangmeng Liu[a], Chuan Zhang[b,*], Peng Sun[a], Xu Yan[a], Geyu Lu[a,*]

[a] State Key Laboratory on Integrated Optoelectronics, Key Laboratory of gas sensors, College of Electronic Science and Engineering, Jilin University, 2699 Qianjin Street, Changchun, Jilin Province, 130012, China
[b] Department of Endocrinology and Metabolism, the Second Hospital of Jilin University, China

ARTICLE INFO

Keywords:
Mixed potential acetone sensor
$Bi_{0.5}La_{0.5}FeO_3$
Exhaled breath
Diabetic ketosis

ABSTRACT

Non-invasive monitoring performed by breath analysis to achieve early diagnosis of diabetic ketosis have attracted widespread attention. In this study, mixed potential type acetone sensors based on $Ce_{0.8}Gd_{0.2}O_{1.95}$ solid electrolyte and $Bi_{1-x}La_xFeO_3$ (x = 0.1, 0.3, 0.5, 0.7, 0.9) sensing electrode (SE) were fabricated successfully and used for the diagnosis of diabetic ketosis through analyzing the concentration of acetone in expiration. The sensor attached with $Bi_{0.5}La_{0.5}FeO_3$-SE presented the highest sensitivity towards acetone among other sensors fabricated in this work, which could detect 1 ppm acetone with the response value of −3 mV. Meanwhile, this sensor showed a relatively high sensitivity of −17.5 mV/decade towards 1–5 ppm acetone at 580 °C. The sensor also displayed excellent repeatability, good selectivity, humidity stability and acceptable long-term stability during 30 days continuously working at 580 °C. Based on the sensing performance of this sensor, the exhalation of diabetics were measured, and results indicated that the sensor used $Bi_{0.5}La_{0.5}FeO_3$-SE exhibited stable and reliable characteristics to the breath tests of diabetics. In addition, a positive correlation relationship between acetone concentration in the exhalation of ketosis patients and the blood ketone level were obtained, and this relationship was consistent with reports from other literatures. Hence, in terms of breath detection, this sensor has the potential to detect diabetic ketosis.

1. Introduction

In the field of medical, some new disease diagnosis methods such as non-invasive diagnostics by human breath analysis have attracted scientists' attention because of their low cost and portable features [1]. In 1970s, More than 200 components was identified in the breath of human using gas chromatography (GC), which marks the beginning of modern respiratory analysis [2,3]. The main components of human exhalation are nitrogen, oxygen, carbon dioxide, water and inert gases. There are also a small fraction composed of more than 1000 volatile organic compounds (VOCs), and the concentrations of these VOCs ranges from parts per million (ppm) to parts per trillion (ppt) by volume [4–6]. Although there are more than 1000 VOCs in the exhalation of human, however, only a few VOCs are common to all the people. These common VOCs, such as acetone, ethane isoprene and methanol, are products of core metabolic processes which could be useful for clinical diagnosis [7].

Diabetes is one of the fastest growing diseases in the world. According to the statistics from World Health Organization (WHO), the number of diabetic patients has quadrupled since 1980, and there will be 552 million diabetic patients all over the world by the year 2030 [8–10]. Diabetes is a lifelong illness that can lead to death and reduce quality of life. It is caused by insufficient insulin production or improper using of insulin in body tissues. Sustained hyperglycemia and long-term metabolic disorders can lead to the damage of the tissues and organs of human body, especially the eyes, kidneys, and cardiovascular, as well as the damage to nervous system and its dysfunction and failure. Some severe patients can cause acute complications such as dehydration, electrolyte imbalance and acid-base balance disorders. Diabetic ketoacidosis (DK) is the late stage of diabetes. When the patient has diabetic ketoacidosis, acetoacetic acid (AcAc), beta-hydroxybutyrate (β−OHB) and acetone in body fluids accumulates. The concentration of AcAc and β−OHB in body fluids causes changes of electrolyte concentration and pH in arterial blood. Meanwhile, spontaneous and non-enzymatic decarboxylation of AcAc increases the concentration of acetone in the blood [11,12]. According to previous reports, acetone

* Corresponding authors.
E-mail addresses: liangxs@jlu.edu.cn (X. Liang), wangs93@sina.com (C. Zhang), lugy@jlu.edu.cn (G. Lu).

https://doi.org/10.1016/j.snb.2019.126688
Received 16 February 2019; Received in revised form 17 May 2019; Accepted 12 June 2019
Available online 12 June 2019
0925-4005/

concentrations in the exhalation of human are related to the ketone content in blood plasma, and β−OHB content in venous blood, therefore, breath acetone and glucose in blood are positive correlated, and this relationship provides effective solution for non-invasive detection of diabetic patients with ketosis [13,14]. It has been reported that in exhalation, the concentration of acetone for the healthy human is 0.3–1 ppm, while, for diabetics patients it is 1–20 ppm or even higher [15,16]. Thus, non-invasive monitoring can be performed by breath analysis to achieve early diagnosis of diabetic ketosis.

Over the years, there have been several methods in the field of breath analysis for the detection of diabetes, such as proton transfer reaction-mass spectroscopy (PTR-MS), gas chromatography/mass spectroscopy (GC/MS), ion mobility spectroscopy (IMS), and selected ion flow tube mass spectroscopy (SIFT-MS) [17–21]. Although these detection technologies have high sensitivity, they are still expensive, bulky, and not portable. In addition, all these methods require longer time for sample preparation, so, they can't achieve real-time monitoring [17]. Gas sensors with the advantages of low cost, miniaturization, portability and high performance have become potential methods to the breath detection for diagnosis of diabetes. A variety of acetone gas sensors based on different working mechanism have been reported. Some resonant chemical sensors, such as surface acoustic wave (SAW), cantilever, quartz crystal microbalance (QCM) and capacitive micromachined ultrasonic transducer (CMUT), have been widely reported [22–25]. These sensors have the advantages of high sensitivity, miniaturization, and they can work at ambient temperature. However, the selectivity of these sensors is usually not good, and the changes of temperature and humidity in the environment also have a great impact on such sensors [25]. Using the unique optical properties of acetone, fluorescent sensors based on metal-organic frameworks (MOF) or coordination polymers (CPS) have been developed to detect acetone [26–28]. Although this kind of acetone sensor has good stability, it couldn't meet the requirement of non-invasive detection because most fluorescent sensors can only detect liquid, and the synthesis methods of fluorescent probes are usually complicated, which limits their application [29]. Among the various of gas sensors, semiconductor oxide acetone sensors and solid electrolyte type acetone sensors are most widely studied [30–34]. Semiconductor oxide sensors usually have a much lower detection limit than other kinds of sensors, while the stability of this type of sensor is not very good. Compared with semiconductor oxide sensors, solid state electrolyte sensors have better accuracy and stability, which provide a reliable guarantee for the application of them. As a commonly used solid electrolyte, yttria-stabilized zirconia (YSZ) have been widely reported, and mixed potential gas sensors based on YSZ solid electrolyte also exhibited good sensing performances in the detection of VOCs. However, from the aspect of practical application, because of the high operating temperature of YSZ-based mixed potential gas sensors [33,34], the power consumption of this kind of sensor is usually higher than other sensors. In recent years, among the solid electrolytes working in the range of middle temperature, CeO_2-based solid-state ionic conductor was extensively examined in the field of solid oxide fuel cell (SOFC). As reported, the conductivity of doped-CeO_2 is one order of magnitude higher than that of YSZ [35]. Therefore, CeO_2-based mixed potential sensors have been gradually studied [36–39], however, there are not much reports on the use of this kind of sensor detect acetone, and it is rare to use for the breath analysis of diabetic patients. Perovskite-type oxides were widely used as sensing materials to fabricate gas sensors because of its high stability at relatively high temperatures [40,41]. And based on the previous works of our group [35–37], CeO_2-based mixed potential sensors attached with perovskite-type oxides such as $La_{0.8}Sr_{0.2}CoO_3$, $SrMnO_3$ and $BiFeO_3$ showed good sensing performance towards acetone. As reported in the literature [42], to La doped $BiFeO_3$ nanoparticles, the La dopants could act as trapping centers of hole or electron, which could facilitate the production and separation of charge carriers and reduce the recombination rate at the same time, hence improve the electrochemical properties of $BiFeO_3$ nanoparticles. Therefore, we chose La doped $BiFeO_3$ as the sensing material to fabricate CeO_2-based mixed potential type acetone gas senor.

In this study, sensors based on $Ce_{0.8}Gd_{0.2}O_{1.95}$ solid electrolyte and $Bi_{1-x}La_xFeO_3$ sensing electrode (SE) were fabricated and used for clinical detection to analyze the amount of acetone in the exhalation of diabetic patients.

2. Experimental

2.1. Preparation and characterization of $Bi_{1-x}La_xFeO_3$ sensing electrode materials

$Bi_{1-x}La_xFeO_3$ (x = 0.1, 0.3, 0.5, 0.7, 0.9) sensing electrode materials were prepared by sol-gel method, using $Bi(NO_3)_3{\cdot}5H_2O$, $La(NO_3)_3{\cdot}6H_2O$, $Fe(NO_3)_3{\cdot}9H_2O$ and citric acid (CA) as raw materials. All chemicals in this paper were of analytical grade and without any further purification. According to a certain stoichiometric ratio (Bi^{3+}: La^{3+}: Fe^{3+} = 1-x: x: 1), three nitrates ($Bi(NO_3)_3{\cdot}5H_2O$, $La(NO_3)_3{\cdot}6H_2O$, $Fe(NO_3)_3{\cdot}9H_2O$) were dissolved in dilute nitric acid under magnetic stirring. CA was fully dissolved in deionized water with the molar ratio of 1:1 to all metal cations (Bi^{3+}, La^{3+} and Fe^{3+}), then dropwise added into the as-prepared nitrate solution with vigorous stirring in water bath of 80 °C to prepare a gel solution. After drying in the electric vacuum of 100 °C for 10 h, amorphous polymeric precursors were formed and then sintered at 800 °C for 2 h to obtain the final materials.

Crystal structures and morphology of the as-prepared $Bi_{1-x}La_xFeO_3$ (x = 0.1, 0.3, 0.5, 0.7, 0.9) sensing electrode materials were performed by X-ray diffraction (XRD) patterns and field-emission scanning electron microscopy (FESEM) patterns. XRD patterns were measured in the range of 20-80° with the Rigaku wide-angle X-ray diffractometer (D/max rA, using Cu Kradiation at wave length = 0.1541 nm). And FESEM patterns were obtained by the JEOL JSM-7500 F microscope at the accelerating voltage of 10 kV. Nanoparticle size and Zeta potentiometer (Zetasizer Nano ZS90) was used to measure the average size of the materials fabricated in this work.

2.2. Fabrication and measurement of gas sensors

Sensors in this paper are all planar structure using $Ce_{0.8}Gd_{0.2}O_{1.95}$ plate (0.2 mm thickness, 2 mm × 2 mm square, provided by Ningbo SOFCMAN Energy Technology Co., Ltd) as solid electrolyte. A platinum dot and a narrow stripe-shaped platinum electrode (reference electrode, RE) were coated on both sides of the $Ce_{0.8}Gd_{0.2}O_{1.95}$ substrate with platinum paste (Sino-platinum Metals Co., Ltd). Then, two pieces of platinum wire were pasted on the platinum point and the platinum stripe, respectively, and sintered the $Ce_{0.8}Gd_{0.2}O_{1.95}$ substrate at 950 °C for half an hour in muffle furnace. After annealing, the as-synthesized sensing materials were mixed with a little deionized water to prepare a slurry and covered on the platinum dot to fabricate a platinum stripe. After sintered at 800 °C for 2 h in muffle furnace to allow the materials to dry sufficiently and adhere tightly to the $Ce_{0.8}Gd_{0.2}O_{1.95}$ substrate, the $Ce_{0.8}Gd_{0.2}O_{1.95}$ plate were fixed to heater consisting of a Al_2O_3 substrate (2 mm × 2 mm square) and two pieces of Pt wire by the inorganic adhesive, where the heater could provide the operating temperature for the sensor. The schematic diagram of the sensor was shown in Fig.1.

A common static test method were used to test sensing properties of the as-fabricated sensors [34]. A constant current source provided by a linear DC Power Supply (Gwinstek GPD-3303S) was used to supply the corresponding current to the heater, and the heater converted the current into heat required for the sensor to keep operating normally. The potential difference between the sensitive electrode and the reference electrode was measured by Digital Multimeter (Fluke 8808A) and stored as the response signal (ΔV) of the sensor in a computer connected to the Digital Multimeter. The polarization curves of the

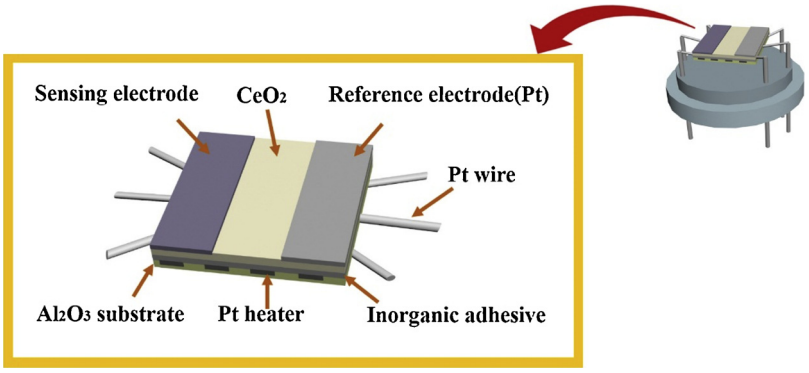

Fig. 1. Schematic diagram of the sensor.

sensor attached with $Bi_{1-x}La_xFeO_3$ (x = 0.1, 0.3, 0.5, 0.7, 0.9) were measured using an electrochemical workstation (Instrument Corporation of Shanghai, China, CHI600C) in 50 ppm acetone at 580 °C.

Different concentrations of VOCs were obtained by the static liquid gas distribution method, which was calculated by the following formula.

$$C = \frac{22.4 \times \rho \times \varphi \times V_1}{M \times V_2} \times 1000$$

Where C (ppm) is the VOCs gas concentration needed; ρ (g/mL) is the density of the VOCs in liquid state; φ is the VOC gas volume fraction; V_1 (L) and M (g/mol) are the volume and molecular weight of liquid VOC, respectively; V_2 (L) is the volume of the chamber.

The exhalation of diabetic patients was collected from the Second Hospital of Jilin University, and all experiments were conducted in accordance with relevant Chinese laws and regulations. We used clean gas-collecting bag to collect the exhalation of diabetic patients, and the specific measure method for this exhalation is as follows: firstly, we pumped an airtight chamber with the volume of 1 L into vacuum, and then, the exhalation was injected into the vacuum chamber by the pressure difference between the gas-collecting bag and the vacuum chamber, finally, the sensor fabricated in this work was placed into the chamber to measure the potential difference between SE and RE.

3. Results and discussion

Powder X-ray diffraction (XRD) was used to measure the crystallographic structure and phase purity of the as-synthesized materials. Fig. 2(a) shows the XRD patterns of $Bi_{1-x}La_xFeO_3$ (x = 0.1, 0.3, 0.5, 0.7, 0.9), $BiFeO_3$ (JCPDS#72-2112) and $LaFeO_3$ (JCPDS#75-439). From the figure we could see that the 2θ corresponding to all main phases of $Bi_{1-x}La_xFeO_3$ were between $BiFeO_3$ and $LaFeO_3$. Fig. 2(b) is the (110) peaks in an expanded scale. It can be seen from that the double split peak is partially weakened and shifted to a higher angle with the increase of La^{3+} concentration which indicated that the rhombohedral structure of $BiFeO_3$ distorted to orthorhombic structure because of the substitution of La^{3+} [43,44].

FESEM micrographs of as-prepared $Bi_{1-x}La_xFeO_3$ (x = 0.1, 0.3, 0.5, 0.7, 0.9) sintered at 800 °C are presented in Fig. 3(a–e) which indicated the effect of La^{3+} doping on the surface morphology and particle size. From which we can see that all the materials performed a porous structure, and with the increase of La^{3+} concentration, the average particle size and porosity of $Bi_{1-x}La_xFeO_3$ decreased gradually. We used Nanoparticle size and Zeta potentiometer (Zetasizer Nano ZS90) to measure the average size of the materials. As shown in Fig.3(f), the average size of the particle was 747.1 nm to $Bi_{0.9}La_{0.1}FeO_3$, 725.5 nm to $Bi_{0.7}La_{0.3}FeO_3$, 699.7 nm to $Bi_{0.5}La_{0.5}FeO_3$, 670.7 nm to $Bi_{0.3}La_{0.7}FeO_3$ and 539.7 nm to $Bi_{0.1}La_{0.9}FeO_3$. The decreased particle size and porosity with the increase of La^{3+} concentration may be caused by the suppression to the grain growth in perovskite. Rare-earth substituted ions of large radius are more difficult to enter the unit cell of crystal lattice and more efficient to suppress the grain growth, which is probably attributed to the lower diffusivity of them [45,46]. Particle size and porosity are two important factors to the sensing performance of sensor, which are closely related with the diffusion of target gas in SE, and we will discuss it in the part of sensing mechanism.

For the purpose of exploring the best substitution of La^{3+}, sensitivity of the sensors attached with $Bi_{1-x}La_xFeO_3$-SE were measured and related results were presented in Fig. 4(a–e). In this study, Sensors used $Bi_{1-x}La_xFeO_3$ (x = 0.1, 0.3, 0.5, 0.7 and 0.9) -SE were named as S1, S3, S5, S7, and S9, respectively. From Fig. 4 we can see that the relationship between the response of the sensor and the logarithm of acetone concentration is segmented linear, and the slope of sensor S5 was the largest among all the sensor fabricated in this work, which were −17.5 mV/decade to 1–5 ppm acetone and −36.7 mV/decade to 5–50 ppm acetone. Therefore, $Bi_{0.5}La_{0.5}FeO_3$ was considered to be the

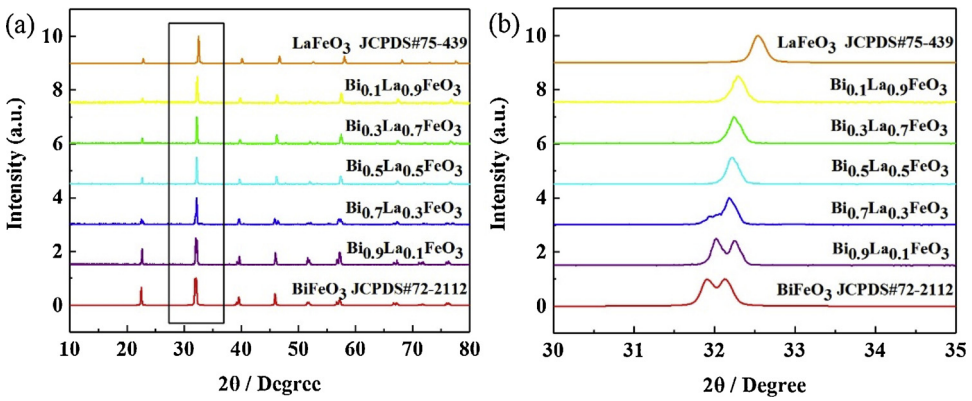

Fig. 2. XRD patterns of $Bi_{1-x}La_xFeO_3$ (x = 0.1, 0.3, 0.5, 0.7, 0.9) sensing materials; (a) 10–80°; (b) 30–35°.

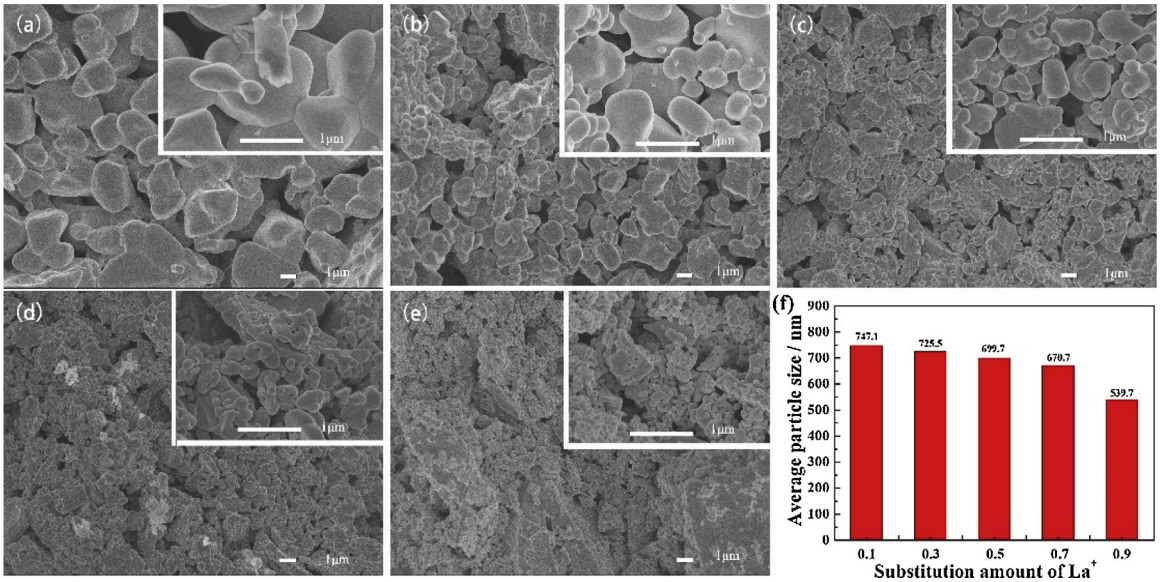

Fig. 3. SEM patterns of $Bi_{1-x}La_xFeO_3$ (x = 0.1, 0.3, 0.5, 0.7, 0.9), (a) x = 0.1; (b) x = 0.3; (c) x = 0.5; (d) x = 0.7; (e) x = 0.9. (f) the average particle size of $Bi_{1-x}La_xFeO_3$ (x = 0.1, 0.3, 0.5, 0.7, 0.9).

best sensing material in this work. We compared the response and sensitivity to acetone of sensors reported in literatures, and recorded in Table 1, it can be seen that sensor S5 fabricated in this work displayed a better sensitivity to 1–5 ppm acetone than other devices.

Sensing mechanism of mixed potential type acetone sensor can be described as follows [34,35]: when the sensor exposed in acetone gas, two progresses took place on the sensing electrode. The diffusion of acetone in SE layer was the first progress, in which oxidation of acetone occurred, resulting in a decrease in the concentration of acetone at the trip-phase-boundary (TPB: sensing electrode/CeO_2/test gas). The second progress was the electrochemical redox reactions (1) and (2) happened at TPB and formed a local cell. The potential at SE was the mixed potential when the two reactions reached to a dynamic equilibrium.

Cathodic reaction: $O_2 + 4e^- \rightarrow 2O^{2-}$ (1)

Anodic reaction: $1/4\ C_3H_6O + 2O^{2-} \rightarrow 3/4CO_2 + 3/4H_2O + 4e^-$ (2)

Sensing performance of the sensor relays on acetone concentrations at TPB, the number of TPB active sites and the electrochemical catalytic activity of sensing material. As shown in Fig. 4, The sensor showed a segmented linear relationship between the response of the sensor and the logarithm of acetone concentration. The possible reason for the piecewise linearity of sensitivity was as follows. For mixed potential sensor, electrochemical reaction occurred at TPB was related to the amount of acetone through SE to TPB and the number of active sites at TPB. To the sensor fabricated with $Bi_{0.5}La_{0.5}FeO_3$-SE, the number of active sites was certain, therefore, for low concentration of acetone, the amount of acetone which diffused through the sensitive electrode layer to TPB and participated in the electrochemical reaction was an important factor affecting the sensitivity of the sensor. However, the consumption of acetone in the diffusion process may reduce the

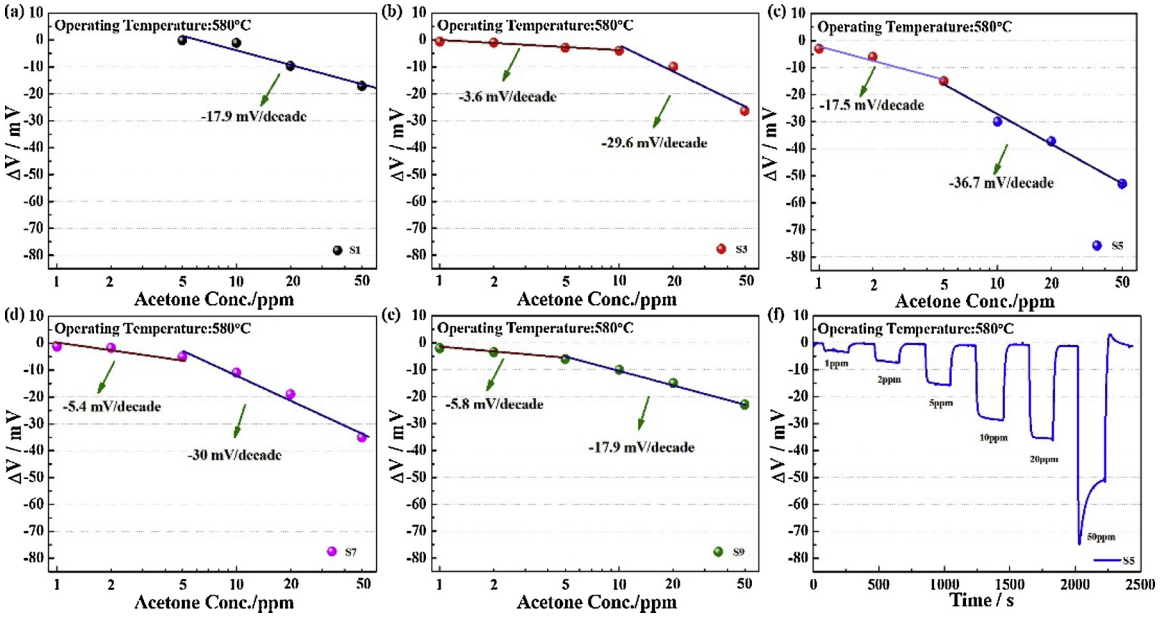

Fig. 4. Dependence of ΔV for the sensor S1-S9 on the acetone concentration at 580 °C, (a) S1; (b) S3; (c) S5; (d) S7; (e) S9; (f) Response transient curves for the sensor S5 to 1–50 ppm acetone at 580 °C.

Table 1
Comparison of the response and sensitivity for different sensors.

Material	Acetone Conc. (ppm)	Response	Sensitivity	Operating temperature(°C)	Ref.
CMUT	2500–25000	–	0.4 Hz/ppm	room temperature	[22]
CNDs	0.1–0.5 vol%	–	0.991	room temperature	[29]
Cd-MOF	0.1–100 vol%	–	–	room temperature	[26]
TiO_2-/SnO_2	10–500	13.7 (100 ppm)	–	280	[30]
SnO_2/α-Fe_2O_3	5–10000	5.6 (5 ppm)	–	200	[31]
NiO-WO_3	20–800	6.6 (20 ppm)	–	375	[32]
$NiNb_2O_6$	0.5–5	−1.2 mV (0.5 ppm)	−13	650	[33]
$Zn_3V_2O_8$	1–10	−2.5 mV (1 ppm)	−16	600	[34]
$Bi_{0.5}La_{0.5}FeO_3$	1–5	−3 mV (1 ppm)	−17.5 mV/decade	580	Present work

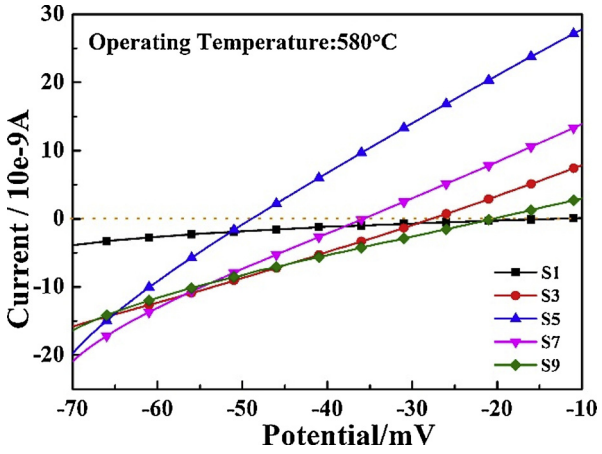

Fig. 5. Polarization curves in air +50 ppm acetone for the sensor attached with $Bi_{1-x}La_xFeO_3$ (x = 0.1, 0.3, 0.5, 0.7, 0.9)-SE.

quantity of acetone reached to TPB, and compared with high concentration of acetone, the proportion of consumption in lower concentration of acetone was more, thus, there was a lower sensitivity for low concentration of acetone. As Fig. 3 shows, the average particle size and porosity of $Bi_{1-x}La_xFeO_3$ decreased with the increase of La^{3+} substitution. The decrease of particle size causes an increase in the effective area of TPB, resulting in an increase in the number of electrochemically reactive active sites at TPB, which could induce a higher sensitivity to the sensor. However, smaller porous channels may increase the consumption of acetone in sensing electrode material, which is not helpful to the gas diffusion. When the two influencing factors are balanced, the sensor may have the best sensitivity to acetone. Additionally, in order to compare the electrochemical catalytic activity of these five materials, polarization curves in air +50 ppm acetone were tested and shown in Fig. 5. The slope of the curve for S5 was the largest among all these five sensors, which indicated that the electrochemical catalytic activity of $Bi_{0.5}La_{0.5}FeO_3$ was the best among all the sensing materials synthesized in this work. Appropriate particle size and porosity as well as the best electrochemical catalytic activity of $Bi_{0.5}La_{0.5}FeO_3$ to acetone, these factors contributed together to the highest responses towards acetone for S5.

As an important parameter in the actual application process, the optimum working temperature was measured and shown in Fig. 6. From which we can see that as the increase of temperature, the sensitivity change of S5 reached to the largest (-17.5 mV/decade) at 580 °C towards the range of 1–5 ppm, −52 mV/decade at 610 °C towards 5–50 ppm acetone. Because this work was mainly for the low concentration acetone in the exhalation of diabetic patients, so we chose 580 °C as optimum working temperature. The response values and sensitivity of the device showed a trend of "increase-maximum-decrease" with the increase of temperatures, and the reason for this phenomenon may be related to activation energy [33]. Definite activation energy is a necessary condition to the smooth occurrence of the electrochemical reaction at TPB. When the temperature was below the optimum working temperature, there was less effective gas collisions, and the number of activated acetone molecules increased with the increase of temperature, which means that more acetone molecules have enough activation energy to participate in the reaction, therefore, the sensitivity of the sensor increased with the increasing of temperature. However, when the temperature continues to increase, the desorption process of acetone at SE played a more important role, and the amount of acetone adsorbed on sensing electrode reduces with the increase of operating temperature, which might be the main reason that the sensitivity of the sensor decreased with the increase of operating temperature.

As the continuous response and recovery transient curves displayed in Fig.7 **(a)**, in six consecutive tests to 2 ppm, 5 ppm and 10 ppm acetone, response values of the sensor attached with $Bi_{0.5}La_{0.5}FeO_3$-SE had small fluctuations, which means that the sensor has excellent repeatability. Additionally, we measured another five sensors used $Bi_{0.5}La_{0.5}FeO_3$-SE (S5-1, S5-2, S5-3, S5-4, S5-5) towards 2 ppm acetone, as shown in Fig.7(b). ΔV_e ($\Delta V_e = \Delta V_n - \Delta V_0$, where ΔV_n and ΔV_0 were the response values of sensor S5-n and S5 to 2 ppm acetone) was used to characterize the difference between these sensors. The maximum value of ΔV_e was 1 mV, which indicated the good reproducibility of the sensors. The excellent repeatability and good reproducibility provide protection together for the practical application of the sensor. Human exhalation contains many different ingredients, therefore, the cross-sensitivities of the sensor towards 10 ppm various gases has been measured, as Fig. 8 shows. Compared with other gases tested in this work, the response value of S5 towards acetone was the highest, and this reveals that the sensor has a good selectivity. The opposite responses among various gases could be explained as follows: to reducing gas, such as acetone, the electrochemical redox reactions (1) and (2) happened at TPB, acetone was the anodic, O^{2-} flowed from GDC to acetone, however, for oxidizing gas, such as NO_2, the reactions happened at TPB were shown in (3) and (4), where NO_2 was the cathodic, O^{2-} flowed from NO_2 to GDC.

$$\text{Cathodic reaction: } NO_2 + 2e^- \rightarrow NO + O^{2-} \quad (3)$$

$$\text{Anodic reaction: } O^{2-} \rightarrow 1/2O_2 + 2e^- \quad (4)$$

In addition, humidity stability and long-term stability of the sensor were also been tested and shown in Fig. 9(a–d). From Fig.9(a) and (b), it can be seen that at the relative humidity of 20%–80%, the change amplitudes of the response values for S5 were about 6.6%–13.2% towards 2 ppm acetone, 10%–12.6% towards 5 ppm acetone and 6.4% to 4.6% towards 10 ppm acetone. This means that the sensor has good humidity stability. The long-term stability of the sensor attached with $Bi_{0.5}La_{0.5}FeO_3$-SE was measured under 30 day's continuous work at 580 °C, the responses of the sensor to 5 ppm and 10 ppm acetone were tested every 5 days. The change amplitude of the ΔV (ΔV_s) was represented by the formula $\Delta V_s = [(\Delta V_n - \Delta V_0)/\Delta V_0 \times 100\%]$, where, ΔV_n and ΔV_0 were the ΔV of S5 on the n day and initial day, respectively. According to Fig. 9(d–e), the sensing performance of the sensor decreased more in the first 5 days, and then stabilized. The ΔV_s of the

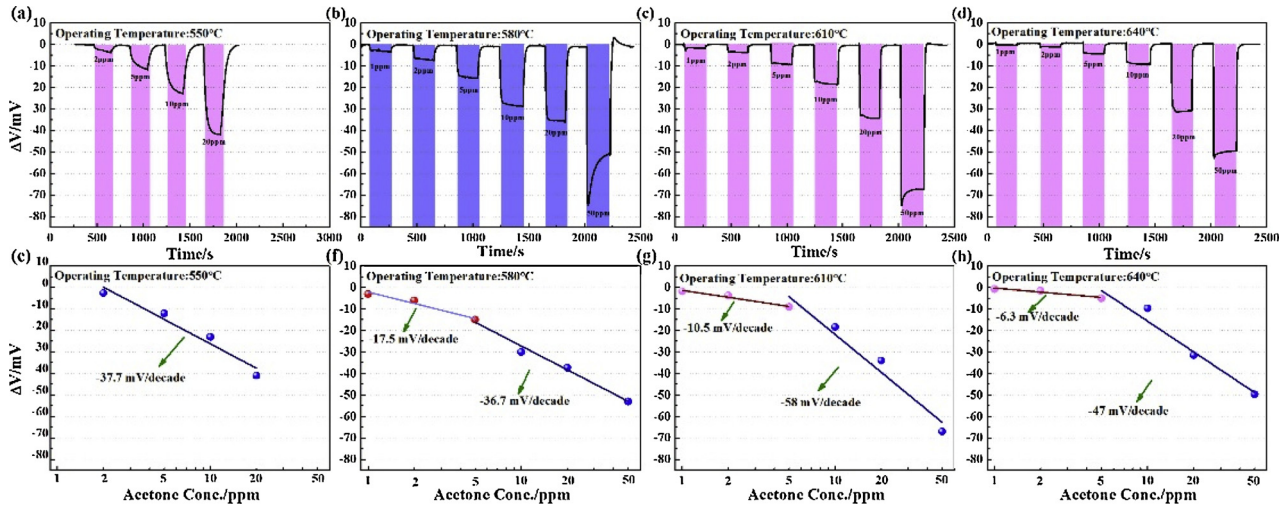

Fig. 6. Response and recovery transients for the sensor S5 towards 1–50 ppm acetone at (a) 550 °C, (b) 580 °C, (c) 610 °C, (d) 640 °C; Dependence of ΔV for the sensor S5 towards 1–50 ppm acetone at (e) 550 °C, (f) 580 °C, (g) 610 °C, (h) 640 °C.

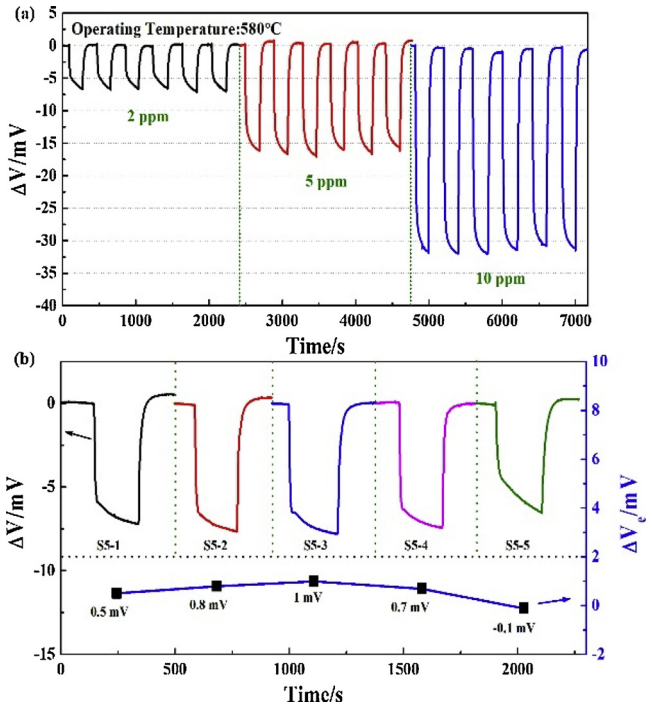

Fig. 7. (a) Continuous response-recovery transients for the sensor S5 to 2 ppm, 5 ppm and 10 ppm acetone; (b) Response transient curves for sensor S5-n (n = 1–5) to 2 ppm acetone.

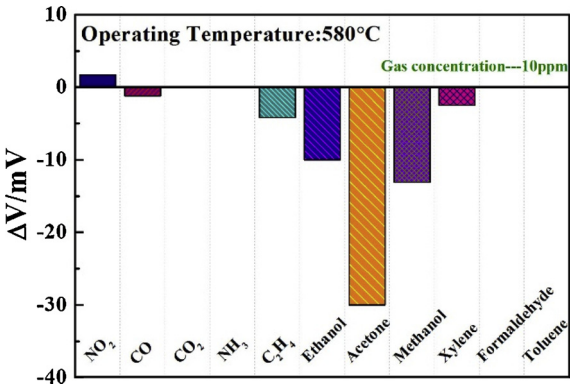

Fig. 8. Cross-sensitivities for the sensor S5 to various gases at 580 °C.

sensor were about 21.6% to 5 ppm acetone and 26.7%–10 ppm acetone on the 30th days, which indicates that the long-term stability of this sensor was not very good, and we could correct the responses of the sensor through intelligent algorithms in clinical detection to ensure that the sensor could output signals stably.

Based on the sensing performance of the sensor we fabricated in this work, we conducted clinical tests for the exhalation of 8 diabetics from the Second Hospital of Jilin University. Among the 8 patients, 2 patients were non-ketotic Type 2 diabetes (T2DM), and the other 6 persons were diabetic ketosis patients. One of the 6 diabetic ketosis patients has a blood ketone concentration of 0.5 mmol/L and is accompanied by urinary ketone +. All the response and recovery curves towards the exhalation of these eight diabetics were measured and shown in Fig. 10(a), from which we can see that the sensor based on $Bi_{0.5}La_{0.5}FeO_3$-SE has distinct and stable signals for exhaled breathing to all the eight patients. Usually, diabetics with the ketone content more than 0.5 mmol/L are ketosis patients, with or without urinary ketone body +. Therefore, we tested the exhalation of the ketosis patient with urinary ketone +, the response value of the sensor towards the exhalation of this patient was about −4 mV, and this value was no significant difference with the patient whose blood ketone concentration was 0.5 mmol/L and without urinary ketone +, which revealed that acetone concentration in the exhalation of the ketosis patients has rare relationship with urinary ketone concentration. In addition, we also tested the responses for sensor S5 to the breath of three healthy people, related results have been shown in Fig.10(b). We can see that the response values of sensor S5 towards the breath of healthy people were -2.1 mV, -3.5 mV and -3.3 mV, which is lower than the acetone concentration in the breath of ketosis patients.

We conducted two clinical tests with a 58-day interval, four diabetics were tested each time. Because of the long interval between these two clinical tests, the sensitivity of the device was recalibrated before the second test to ensure the accuracy of the experiment results. Fig. 11(a) and (b) show the sensitivity curves of the sensor before these two clinical tests, and the black points on the sensitivity curves represent the ΔV towards the exhalation of these eight diabetics. ΔV of the sensor to the exhalation of the two non-ketotic diabetic patients were -3.6 mV and -4.8 mV, and the acetone concentration were 0.78 ppm and 1 ppm. ΔV of the sensor towards ketosis patients were higher than that of non-ketotic patients, which means that the senor fabricated in this work could distinct ketosis patients from all diabetics. Furthermore, as Fig. 11(c) displayed, we obtained the relationship

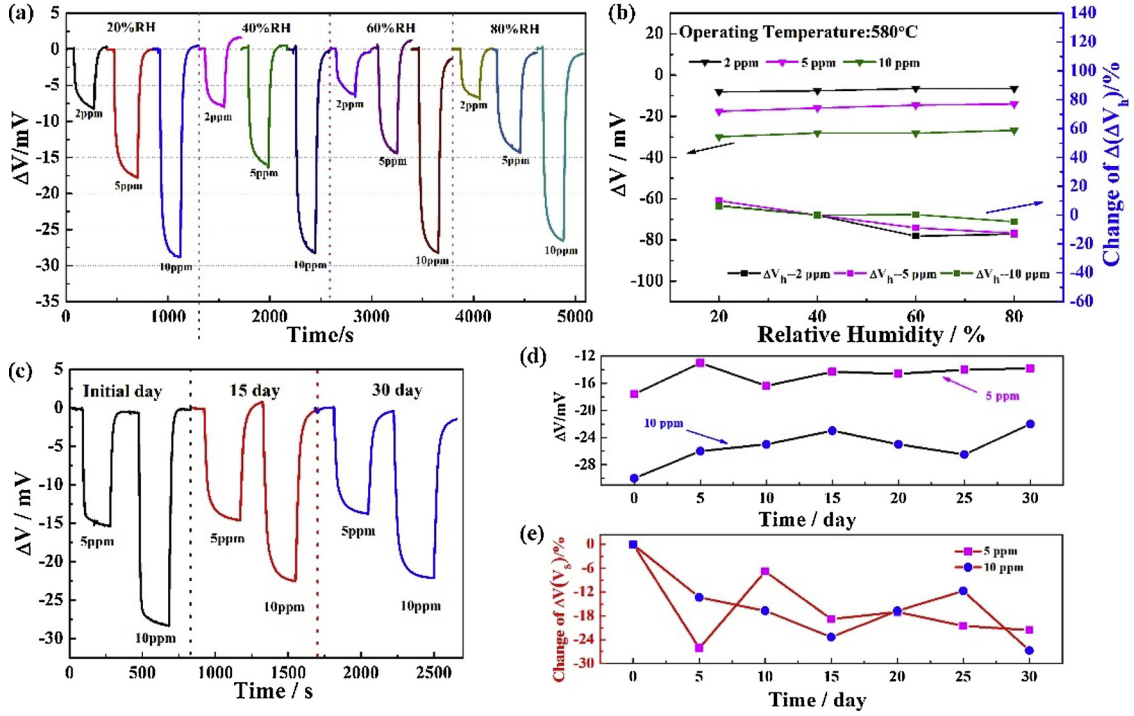

Fig. 9. (a) Response and recovery transients for the sensor S5 to 2 ppm, 5 ppm and 10 ppm acetone under different relative humidity at 580 °C; (b) Response of the sensor S5 to 2 ppm, 5 ppm and 10 ppm acetone under different relative humidity; (c) Response and recovery transients for the sensor S5 to 5 and 10 ppm acetone on the 0th, 15th, 30th days; (d) Response values to 5 ppm and 10 ppm acetone for the sensor during 30 days; (e) Change amplitudes to 5 ppm and 10 ppm acetone during 30 days.

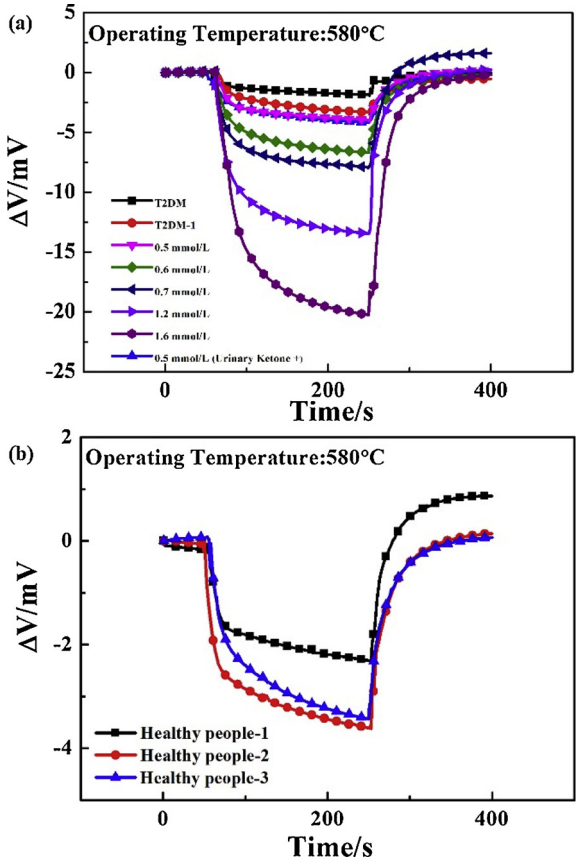

Fig. 10. (a) Response and recovery transient curves for the sensor S5 to the exhalation of the patients with different blood ketone levels; (b) Response and recovery transient curves for the sensor S5 to the exhalation of healthy people.

between acetone concentration and blood ketone level towards five ketosis patients, which could be expressed by the following equation:

$$y = -1.1 + 4.82x$$

Where, x represents blood ketone level, y is acetone concentration. This positive correlation relationship between acetone concentration in the exhalation of ketosis patients and the blood ketone level kept alignment with related results obtained in other reports [11,47]. In conclusion, the sensor fabricated in this work exhibited stable and reliable characteristics to the breath tests of diabetics, which reveals that our sensor could be used as a potential device to monitor acetone in the field of diagnose diabetes with ketosis.

4. Conclusion

In this work, mixed potential type acetone sensor based on CeO_2 solid electrolyte and $Bi_{1-x}La_xFeO_3$ (x = 0.1, 0.3, 0.5, 0.7 and 0.9) sensing electrode were fabricated and used to measure acetone concentration in the exhalation of diabetics. All the sensing materials were synthesized by sol-gel method and sintered at 800 °C. The sensor (S5) attached with $Bi_{0.5}La_{0.5}FeO_3$-SE displayed the best sensitivity towards 5–50 ppm acetone among all the other sensors fabricated in this work. Meanwhile, this sensor also showed a high sensitivity of −17.5 mV/decade towards 1–5 ppm acetone at 580 °C, and the response value of the sensor to 1 ppm acetone was -3 mV. Besides, the sensor S5 displayed excellent repeatability, good selectivity, humidity stability and acceptable long-term stability during 30 days of continuous work at 580 °C. In addition, the exhalation of non-ketotic diabetics and ketosis patients were measured using the sensor S5, the results showed a positive correlation relationship between acetone concentration and the blood ketone level in the exhalation of ketosis patients, which reveals that our sensor has the ability to detect acetone in the breath of ketosis patients, and it could be a potential device to monitor diabetes with ketosis through breath analysis.

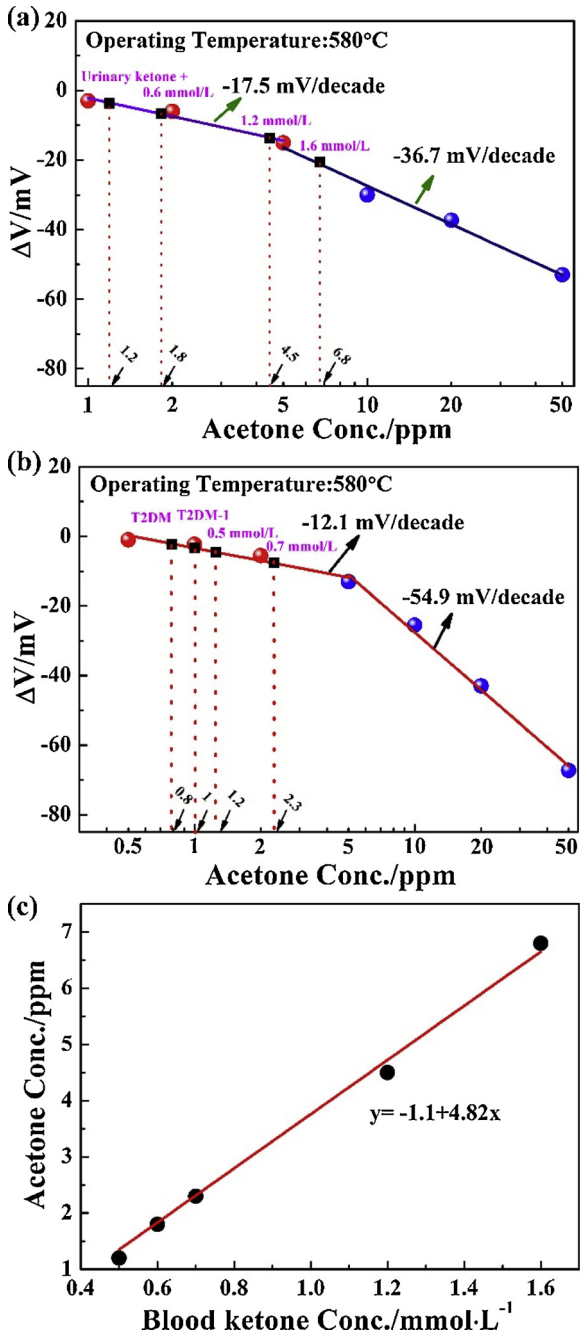

Fig. 11. Location map of breath measurement results on the sensitivity curves of the sensor S5, (a) the first measurement; (b) the second measurement after 58 days; (c) Dependence of acetone concentration on the blood ketone concentration though the test by the sensor S5.

Acknowledgements

This work was supported by the National Nature Science Foundation of China (Nos. 61473132, 61533021 and 61520106003), National Key R&D Program of China (No. 2016YFC0201002) and Program for Chang Jiang Scholars and Innovative Research Team in University (No. IRT-17R47), Application and Basic Research of Jilin Province (20130102010JC), STIRT-JLU (2017TD-07), Graduate Innovation Fund of Jilin University (101832018C015).

References

[1] M. Righettoni, A. Tricoli, Toward portable breath acetone analysis for diabetes detection, J. Breath Res. 5 (2011).
[2] L. Pauling, A.B. Robinson, R. Teranishi, P. Cary, Quantitative analysis of urine vapor and breath by gas-liquid partition chromatography, Proc. Natl. Acad. Sci. U.S.A. 68 (1971) 2374–2376.
[3] W. Miekisch, J.K. Schubert, G.F. Noeldge-Schomburg, Diagnostic potential of breath analysis–focus on volatile organic compounds, Clin. Chim. Acta 347 (2004) 25–39.
[4] W. Cao, Y. Duan, Breath analysis: potential for clinical diagnosis and exposure assessment, Clin. Chem. 52 (2006) 800–811.
[5] M. Phillips, J. Herrera, S. Krishnan, M. Zain, J. Greenberg, R.N. Cataneo, Variation in volatile organic compounds in the breath of normal humans, Journal of chromatography B, Biomed. Sci. Appl. 729 (1999) 75–88.
[6] J.K. Schubert, W. Miekisch, K. Geiger, G.F. Noldge-Schomburg, Breath analysis in critically ill patients: potential and limitations, Expert Rev. Mol. Diagn. 4 (2004) 619–629.
[7] R. Mukhopadhyay, Dont waste your breath, Anal. Chem. 76 (2004) 273a–276a.
[8] A. Takian, S. Kazempour-Ardebili, Diabetes Dictating, Policy: an editorial commemorating world health day 2016, Int. J. Health Policy Manag. 5 (2016) 571–573.
[9] E.G. Krug, Trends in diabetes: sounding the alarm, Lancet 387 (2016) 1485–1486.
[10] C.F. So, K.S. Choi, T.K. Wong, J.W. Chung, Recent advances in noninvasive glucose monitoring, Med. Devices 5 (2012) 45–52.
[11] O.E. Owen, V.E. Trapp, C.L. Skutches, M.A. Mozzoli, R.D. Hoeldtke, G. Boden, et al., Acetone metabolism during diabetic ketoacidosis, Diabetes 31 (1982) 242–248.
[12] A.A.S. Rabih, J.O. Dennis, A.Y. Ahmed, M.H.M. Khir, M.G.A. Ahmed, A. Idris, et al., MEMS-based acetone vapor sensor for non-invasive screening of diabetes, IEEE Sens. J. 18 (2018) 9486–9500.
[13] C. Wang, A.B. Surampudi, An acetone breath analyzer using cavity ringdown spectroscopy: an initial test with human subjects under various situations, Meas. Sci. Technol. 19 (2008).
[14] V. Ruzsanyi, M.P. Kalapos, Breath acetone as a potential marker in clinical practice, J. Breath Res. 11 (2017).
[15] C.J. Wang, A. Mbi, M. Shepherd, A study on breath acetone in diabetic patients using a cavity ringdown breath analyzer: exploring correlations of breath acetone with blood glucose and glycohemoglobin A1C, IEEE Sens. J. 10 (2010) 54–63.
[16] W.W. Li, Y. Liu, X.Y. Lu, Y.P. Huang, Y. Liu, S.Q. Cheng, et al., A cross-sectional study of breath acetone based on diabetic metabolic disorders, J. Breath Res. 9 (2015) 016005.
[17] D.M. Guo, D. Zhang, N.M. Li, L. Zhang, J.H. Yang, A novel breath analysis system based on electronic olfaction, IEEE Trans. Inf. Technol. Biomed. 57 (2010) 2753–2763.
[18] C.H. Deng, J. Zhang, X.F. Yu, W. Zhang, X.M. Zhang, Determination of acetone in human breath by gas chromatography-mass spectrometry and solid-phase microextraction with on-fiber derivatization, J. Chromatogr. B 810 (2004) 269–275.
[19] M. Righettoni, A. Tricoli, S.E. Pratsinis, Si:WO_3 sensors for highly selective detection of acetone for easy diagnosis of diabetes by breath analysis, Anal. Chem. 82 (2010) 3581–3587.
[20] W. Hu, Breath ethanol and acetone as indicators of serum glucose levels: an initial report, Ethnic Dis. 15 (2005) 32–34.
[21] K. Musa-Veloso, S.S. Likhodii, S.C. Cunnane, Breath acetone is a reliable indicator of ketosis in adults consuming ketogenic meals, Am. J. Clin. Nutr. 76 (2002) 65–70.
[22] F.A. Bahos, A. Sainz-Vidal, C. Sanchez-Perez, J.M. Saniger, I. Gracia, M.M. Saniger-Alba, et al., ZIF nanocrystal-based surface acoustic wave (SAW) electronic nose to detect diabetes in human breath, BiosensorsBasel 9 (2018) 4.
[23] A. Gupta, T.S. Singh, R.D.S. Yadava, MEMS sensor array-based electronic nose for breath analysis-a simulation study, J. Breath Res. 13 (2019) 016003.
[24] K.N. Chappanda, M.R. Tchalala, O. Shekhah, S.G. Surya, M. Eddaoudi, K.N. Salama, A Comparative Study of Interdigitated Electrode and Quartz Crystal Microbalance Transduction Techniques for Metal-Organic Framework-Based Acetone Sensors, SensorsBasel 18 (2018) 3898.
[25] I. Yoon, G. Eom, S. Lee, B.K. Kim, S.K. Kim, H.J. Lee, A capacitive micromachined ultrasonic transducer-based resonant sensor array for portable volatile organic compound detection with wireless systems, Sensors Basel (Basel) 19 (2019) 1401.
[26] F.Y. Yi, W.T. Yang, Z.M. Sun, Highly selective acetone fluorescent sensors based on microporous Cd(II) metal-organic frameworks, J. Mater. Chem. 22 (2012) 23201–23209.
[27] H.N. Wang, S.Q. Jiang, Q.Y. Lu, Z.Y. Zhou, S.P. Zhuo, G.G. Shan, et al., A pillar-layer MOF for detection of small molecule acetone and metal ions in dilute solution, RSC Adv. 5 (2015) 48881–48884.
[28] S. Dang, X. Min, W. Yang, F.Y. Yi, H. You, Z.M. Sun, Lanthanide metal-organic frameworks showing luminescence in the visible and near-infrared regions with potential for acetone sensing, Chemistry 19 (2013) 17172–17179.
[29] L. Sai, X. Wang, Q. Chang, W. Shi, L. Huang, Selective determination of acetone by carbon nanodots based on inner filter effect, Spectrochimica acta Part A, Mol. Biomol. Spectr. 216 (2019) 290–295.
[30] F. Li, X. Gao, R. Wang, T. Zhang, G.Y. Lu, Study on TiO_2-SnO_2 core-shell heterostructure nanofibers with different work function and its application in gas sensor, Sensor Actuat. B-Chem. 248 (2017) 812–819.
[31] C.H. Zhao, W.Q. Hu, Z.X. Zhang, J.Y. Zhou, X.J. Pan, E.Q. Xie, Effects of SnO_2 additives on nanostructure and gas-sensing properties of alpha-Fe_2O_3 nanotubes, Sensor Actuat. B-Chem. 195 (2014) 486–493.
[32] J.N. Zhang, H.B. Lu, C. Liu, C.J. Chen, X. Xin, Porous NiO-WO_3 heterojunction nanofibers fabricated by electrospinning with enhanced gas sensing properties, RSC Adv. 7 (2017) 40499–40509.
[33] F.M. Liu, X. Yang, B. Wang, Y.H. Guan, X.S. Liang, P. Sun, et al., High performance mixed potential type acetone sensor based on stabilized zirconia and $NiNb_2O_6$ sensing electrode, Sensor Actuat. B-Chem. 229 (2016) 200–208.
[34] F.M. Liu, Y.H. Guan, R.Z. Sun, X.S. Liang, P. Sun, F.M. Liu, et al., Mixed potential

type acetone sensor using stabilized zirconia and $M_3V_2O_8$ (M: Zn, Co and Ni) sensing electrode, Sensor Actuat. B-Chem. 221 (2015) 673–680.
[35] X. Yang, X.D. Hao, T. Liu, F.M. Liu, B. Wang, C. Ma, et al., CeO_2-based mixed potential type acetone sensor using $La_{1-x}Sr_xCoO_3$ sensing electrode, Sensor Actuat B-Chem. 269 (2018) 118–126.
[36] T. Liu, X. Yang, C. Ma, X.D. Hao, X.S. Liang, F.M. Liu, et al., CeO_2-based mixed potential type acetone sensor using $MMnO_3$ (M: Sr, Ca, La and Sm) sensing electrode, Solid State Ion. 317 (2018) 53–59.
[37] T. Liu, Y.Y. Zhang, X. Yang, X.D. Hao, X.S. Liang, F.M. Liu, et al., CeO_2-based mixed potential type acetone sensor using $MFeO_3$ (M: Bi, La and Sm) sensing electrode, Sensor Actuat B-Chem. 276 (2018) 489–498.
[38] J.J. Zhang, C. Zhang, J.F. Xia, Q. Li, D.Y. Jiang, X.H. Zheng, Mixed-potential NH_3 sensor based on $Ce_{0.8}Gd_{0.2}O_{1.9}$ solid electrolyte, Sensor Actuat B-Chem. 249 (2017) 76–82.
[39] R. Mukundan, E.L. Brosha, D.R. Brown, F.H. Garzon, Ceria-electrolyte-based mixed potential sensors for the detection of hydrocarbons and carbon monoxide, Electrochem. Solid St. 2 (1999) 412–414.
[40] M. Siemons, A. Leifert, U. Simon, Preparation and gas sensing characteristics of nanoparticulate p-type semiconducting LnFeO(3) and LnCrO(3) materials, Adv. Funct. Mater. 17 (2007) 2189–2197.
[41] J.W. Fergus, Perovskite oxides for semiconductor-based gas sensors, Sensor Actuat B-Chem. 123 (2007) 1169–1179.
[42] B.P. Reddy, M.C. Sekhar, B.P. Prakash, Y. Suh, S.H. Park, Photocatalytic, magnetic, and electrochemical properties of La doped $BiFeO_3$ nanoparticles, Ceram. Int. 44 (2018) 19512–19521.
[43] B. Yotburut, P. Thongbai, T. Yamwong, S. Maensiri, Electrical and nonlinear current-voltage characteristics of La-doped $BiFeO_3$ ceramics, Ceram. Int. 43 (2017) 5616–5627.
[44] L. Yuan, A.J. Han, M.Q. Ye, X.X. Chen, L.Y. Yao, C. Ding, Synthesis and characterization of environmentally benign inorganic pigments with high NIR reflectance: lanthanum-doped $BiFeO_3$, Dye. Pigment. 148 (2018) 137–146.
[45] Q. Zhang, X.H. Zhu, Y.H. Xu, H.B. Gao, Y.J. Xiao, D.Y. Liang, et al., Effect of La^{3+} substitution on the phase transitions, microstructure and electrical properties of $Bi_{1-x}La_xFeO_3$ ceramics, J. Alloys. Compd. 546 (2013) 57–62.
[46] X.J. Chou, J.W. Zhai, H.T. Jiang, X. Yao, Dielectric properties and relaxor behavior of rare-earth (La, Sm, Eu, Dy, Y) substituted barium zirconium titanate ceramics, J. Appl. Phys. 102 (2007).
[47] V. Ruzsanyi, M.P. Kalapos, Breath acetone as a potential marker in clinical practice, J. Breath Res. 11 (2017) 024002.